NUCLEAR THEORY, Vol. 35 (2016)
eds. M. Gaidarov, N. Minkov, Heron Press, Sofia

Influence of Core Excitation in the Description of Reactions with Halo Nuclei

R. de Diego[1], **A.M. Moro**[2], **J.A. Lay**[3], **J.M. Arias**[2]

[1]Centro de Ciências e Tecnologias Nucleares, Instituto Superior Técnico, Universidade de Lisboa, Estrada Nacional 10 (Km 139,7), P-2695–066 Bobadela LRS, Portugal

[2]Departamento de FAMN, Facultad de Física, Universidad de Sevilla, Apdo. 1065, E-41080 Sevilla, Spain

[3]Dipartimento di Fisica e Astronomia, Università di Padova, I-35131 Padova, Italy and Istituto Nazionale di Fisica Nucleare, Sezione di Padova, I-35131 Padova, Italy

Abstract. We discuss the effect of core excitation in the scattering and breakup of a two-body halo nucleus on several targets. The structure of the projectile is described in the weak-coupling limit, assuming a particle-rotor model. This Hamiltonian is diagonalized in a finite and square-integrable basis of pseudostates whose radial functions result from applying a transformation to the harmonic oscillator basis. This method (THO) is combined with a reaction formalism (XCDCC) which takes into account dynamic core excitation. Under this framework, we consider the scattering of the halo nucleus ^{11}Be on ^{1}H, ^{64}Zn, and ^{208}Pb targets, comparing with available data for these reactions.

1 Introduction

Nuclei in the proximity of the proton and neutron drip-lines are often weakly bound, or even unbound, and hence their properties are influenced by positive-energy states. Collisions of these systems with stable nuclei will also be influenced by the coupling to the unbound states. This effect was first noticed in deuteron-induced reactions, and later observed in the scattering of other loosely bound nuclei, such as halo nuclei. Several formalisms have been developed to account for the effects of the coupling to breakup channels on reaction observables: Continuum-Discretized Coupled-Channels (CDCC) method [1,2], the adiabatic approximation [3, 4], the Faddeev/AGS equations [5, 6], and a variety of semi-classical approximations [7–12].

Typically, these approaches make use of a few-body description of the weakly bound nucleus. Furthermore, in their standard formulations, the constituent fragments are considered to be inert and, therefore, possible excitations of them are ignored. Moreover, bound and unbound states of the few-body system are considered to be well described by pure single-particle configurations. This approximation ignores possible admixtures of different core states in the wave functions

of the complete projectile. These admixtures are known to be important, particularly in the case of well-deformed cores, as for example in the ^{11}Be halo nucleus.

A first attempt to incorporate core excitation effects within a coupled-channels calculation was done in Ref. [13], where the XCDCC formalism was derived as an extension of the CDCC method. Recently, the XCDCC has been combined with the THO approach [14] in order to incorporate a pseudostates (PS) basis in the formalism [15].

Within the CDCC and XCDCC formalisms, the breakup cross sections are described in the c.m. frame, using two-body kinematics. Because of this, the experimental data should be transformed to this frame, an ambiguous process for inclusive data. Furthermore, recent advances at the radioactive beam facilities have opened the possibility to perform exclusive breakup measurements with unstable nuclei. This will require extensions of reaction frameworks and, for the specific case of the CDCC formalism, fivefold fully exclusive cross sections were already derived in [16]. However, a study of exclusive observables in the laboratory frame with core excitation has never been addressed and this will be the main purpose of a forthcoming paper [17]. In this work we present the results within the XCDCC+THO framework [15] for breakup reactions of ^{11}Be on several targets at low and intermediate energies in the c.m frame.

The manuscript is structured as follows. In Section 2 we briefly recall the THO basis to describe two-body loosely-bound systems with core excitation. In Section 3, we review the XCDCC approach and we include the main results for ^{11}Be breakup reactions in Section 4. Finally, we summarize and conclude in Section 5.

2 Structure of the Projectile

We consider a two-body composite projectile, made of a valence particle coupled to a core nucleus, so the Hamiltonian of the system, H_p, can be described in the weak-coupling limit:

$$H_p(\vec{r},\xi) = T(\vec{r}) + V_{vc}(\vec{r},\xi) + h_c(\xi), \tag{1}$$

where $T(\vec{r})$, V_{vc}, and $h_c(\xi)$ refer to the core-valence kinetic energy operator, the valence-core interaction, and the intrinsic Hamiltonian of the core, respectively.

Therefore, the projectile states are expanded as a superposition of products of single-particle configurations and core states. We also assume in the calculations that the core nucleus has a permanent axially symmetric deformation and the surface radius in the body-fixed frame is parameterized as $R(\hat{\xi}) = R_0[1 + \beta_2\, Y_{20}(\hat{\xi})]$, with R_0 an average radius and β_2 the deformation parameter [18]. Starting from a central potential, $V_{vc}^{(0)}(r)$, the full valence-core interaction is obtained by deforming this interaction as,

$$V_{vc}(\vec{r},\hat{\xi}) = V_{vc}^{(0)}\left(r - \delta_2 Y_{20}(\hat{\xi})\right), \tag{2}$$

with $\delta_2 = \beta_2 R_0$. The transformation to the laboratory frame through the rotation matrices $\mathcal{D}^{\lambda}_{\mu 0}(\alpha, \beta, \gamma)$ (depending on the Euler angles $\{\alpha, \beta, \gamma\}$), and the subsequent expansion in spherical harmonics, yields the following potential (see e.g. Ref. [19]):

$$V_{vc}(r, \theta, \phi) = \sqrt{4\pi} \sum_{\lambda\mu} \mathcal{V}^{\lambda}_{vc}(r) \mathcal{D}^{\lambda}_{\mu 0}(\alpha, \beta, \gamma) Y_{\lambda\mu}(\hat{r}), \tag{3}$$

where the radial form factors are given by:

$$\mathcal{V}^{\lambda}_{vc}(r) = \frac{\sqrt{2\lambda+1}}{2} \int_{-1}^{1} V_{vc}\left(r - \delta_2 Y_{20}(\theta', 0)\right) P_{\lambda}(\cos\theta') \, \mathrm{d}\cos\theta'. \tag{4}$$

The eigenstates and the corresponding wavefunctions are obtained by diagonalizing the Hamiltonian in a finite basis of N square integrable functions:

$$\phi^{THO}_{i,\alpha,J_p,M_p}(\vec{r}, \xi) = \frac{R^{THO}_{i,\ell}(r)}{r} \left[\mathcal{Y}_{(\ell s)j}(\hat{r}) \otimes \varphi_I(\xi)\right]_{J_p M_p}, \tag{5}$$

where the index i specifies the basis function (with $i = 1, \ldots, N$) and the label α denotes the set of quantum numbers $\{\ell, s, j, I\}$, with $\vec{\ell}$ (valence-core orbital angular momentum) and $\vec{s}$ (spin of the valence) both coupled to $\vec{j}$ (total valence particle angular momentum). The total spin of the projectile, $\vec{J}_p$, is given by the coupling between $\vec{j}$ and $\vec{I}$ (intrinsic spin of the core). The radial, $R^{THO}_{i,\ell}(r)$, and angular parts, $\mathcal{Y}_{(\ell s)j}(\hat{r})$, describe the valence-core relative motion, while the functions $\varphi_I(\xi)$ correspond to the core states. The functions $R^{THO}_{i,\ell}(r)$ are generated by applying a local scale transformation (LST) to the spherical HO basis functions,

$$R^{THO}_{i,\ell}(r) = \sqrt{\frac{ds}{dr}} \, R^{HO}_{i,\ell}[s(r)], \tag{6}$$

where $R^{HO}_{i,\ell}[s(r)]$ results from the composition of the radial part of the HO functions and the LST, $s(r)$, whose expression follows the analytical prescription in [20]

$$s(r) = \frac{1}{\sqrt{2}b} \left[\left(\frac{1}{r}\right)^m + \left(\frac{1}{\gamma\sqrt{r}}\right)^m\right]^{-\frac{1}{m}}, \tag{7}$$

that depends on the parameters m, γ and the oscillator length b. Nevertheless, according to Ref. [20], the transformation shows a weak dependence on m. Thus, we set this parameter to the value $m = 4$ proposed in [20] and the adopted LST depends actually on γ and b.

The eigenstates of the Hamiltonian (1) are expanded in terms of the THO basis functions,

$$\Phi^{(N)}_{n,J_p,M_p}(\vec{r}, \xi) = \sum_{i=1}^{N} \sum_{\alpha} C^{n}_{i,\alpha,J_p} \frac{R^{THO}_{i,\ell}(r)}{r} \left[\mathcal{Y}_{(\ell s)j}(\hat{r}) \otimes \varphi_I(\xi)\right]_{J_p M_p}, \tag{8}$$

where n is an index identifying each eigenstate and C^n_{i,α,J_p} are the expansion coefficients of the pseudostates in the truncated basis. The corresponding eigenvalues are identified with the energies of bound or continuum states, giving rise to a discrete representation of the energy spectrum.

3 Reaction Formalism: XCDCC Method

The formalism has been presented in detail in Ref. [15] so we just summarize here the main formulae. The three-body wave functions Ψ_{J_T,M_T} are expressed in terms of the set of projectile eigenstates $\{\Phi^{(N)}_{n,J_p}\}$:

$$\Psi_{J_T,M_T}(\vec{R},\vec{r},\xi) = \sum_\beta \chi^{J_T}_\beta(R)\left[Y_L(\hat{R})\otimes\Phi^{(N)}_{n,J_p}(\vec{r},\xi)\right]_{J_T,M_T}, \qquad (9)$$

where $\vec{R}$ stands for the relative coordinate between the projectile center of mass and the target (assumed to be structureless and spinless) while the different quantum numbers are labeled by $\beta=\{L,J_p,n\}$, with $\vec{L}$ (projectile-target orbital angular momentum) and $\vec{J}_p$ both couple to the total spin of the three-body system $\vec{J}_T$, once the spin of the target is ignored.

Upon inserting (9) in the Schrödinger equation, the coefficients $\chi^{J_T}_\beta(R)$ can be calculated from the system of coupled differential equations, whose main ingredients are the coupling potentials:

$$U^{J_T}_{\beta,\beta'}(R) = \langle\beta; J_T|V_{ct}(\vec{R},\vec{r},\xi)+V_{vt}(\vec{R},\vec{r})|\beta'; J_T\rangle\,. \qquad (10)$$

The valence particle-target interaction (V_{vt}) is assumed to be central, and will be represented by a phenomenological optical potential, while the core-target interaction (V_{ct}) is assumed to contain a non-central part, responsible for the dynamic core excitation/deexcitation mechanism. In general, this interaction can be expressed in the form:

$$V_{ct}(\vec{R},\vec{r},\xi) = \sqrt{4\pi}\sum_{Qq} V_{Qq}(r_c,\xi)\,Y_{Qq}(\hat{r}_c), \qquad (11)$$

where $\vec{r}_c=\vec{R}-m_v/(m_v+m_c)\vec{r}$, with m_c and m_v the core and valence particle masses, respectively. Furthermore, in the rotational model assumed here, the multipole terms $V_{Qq}(r_c,\xi)$ factorize into a radial part and a structure part, i.e.,

$$V_{ct}(\vec{R},\vec{r},\xi) = \sqrt{4\pi}\sum_{Qq} \mathcal{V}^Q_{ct}(r_c)\,\mathcal{T}^*_{Qq}(\xi)\,Y_{Qq}(\hat{r}_c). \qquad (12)$$

The matrix elements (10) were explicitly evaluated in Ref. [13]:

$$U^{J_T}_{\beta:\beta'}(R) = \hat{L}\hat{L}'\hat{J}_p\hat{J}'_p(-1)^{J_p+J_T}\sum_\Lambda(-1)^\Lambda\hat{\Lambda}^2 \times\begin{pmatrix}\Lambda & L & L'\\ 0 & 0 & 0\end{pmatrix}\begin{Bmatrix}J_p & J'_p & \Lambda\\ L' & L & J_T\end{Bmatrix}F^\Lambda_{J_p n:J'_p n'}(R)\,. \qquad (13)$$

The radial dependence is given by the form factors $F^{\Lambda}_{J_p n:J'_p n'}(R)$ which, in addition to geometric coefficients, contain the structure reduced matrix elements $\langle I \| \mathcal{T}_Q(\xi) \| I' \rangle$.

For the Coulomb part of the core-target interaction, we use the usual multipole expansion

$$V_{ct}^{\rm coul}(\vec{r}_c, \xi) = \sum_{Q,q} \frac{4\pi}{2Q+1} \frac{Z_t e}{r_c^{Q+1}} \mathcal{M}(EQq)\, Y_{Qq}(\hat{r}_c), \tag{14}$$

where $\mathcal{M}(EQq)$ is the multipole electric operator. Comparing with the general expression (11) we have

$$V_{Qq}(r_c, \xi) \equiv \frac{\sqrt{4\pi}}{2Q+1} \frac{Z_t e}{r_c^{Q+1}} \mathcal{M}(EQq). \tag{15}$$

For the nuclear part of the core-target interaction, we follow the same approach as for the valence-core interaction.

4 Application to ^{11}Be Reactions

The formalism presented has been previously applied to the scattering of the halo nucleus ^{11}Be on several targets and the results compared with the available experimental data in Ref. [15]. We refer to this work for further details about the potentials and we focus on the main features of the reactions on the different targets.

4.1 ^{11}Be+ p resonant breakup

The XCDCC + THO method was applied to the breakup of ^{11}Be on a proton target at 63.7 MeV/nucleon giving the results in Figure 1, where the solid line corresponds to the full calculation. Considering the experimental data [21], the agreement is fairly reasonable, except for the first data point in the higher energy interval.

With the aim of studying the dynamic core excitation effects we also computed the cross sections without the $Q = 2$ term in the nuclear part of the core-target interaction, but keeping the deformation in the neutron-core interaction (dotted line). This result differs significantly from the full calculation and the difference is particularly noticeable in the higher energy interval, due to the dominance of the $3/2^+$ resonance, which is mostly populated by a core excitation mechanism [22].

4.2 ^{11}Be+ ^{64}Zn elastic and breakup

In the case of ^{11}Be+p breakup, the deformed part of the core-target interaction gives rise to an increase of the breakup cross sections. We show now the effect of these terms in the ^{11}Be+^{64}Zn reaction at 28.7 MeV, for which quasi-elastic (elastic + inelastic) data have been reported in Ref. [23].

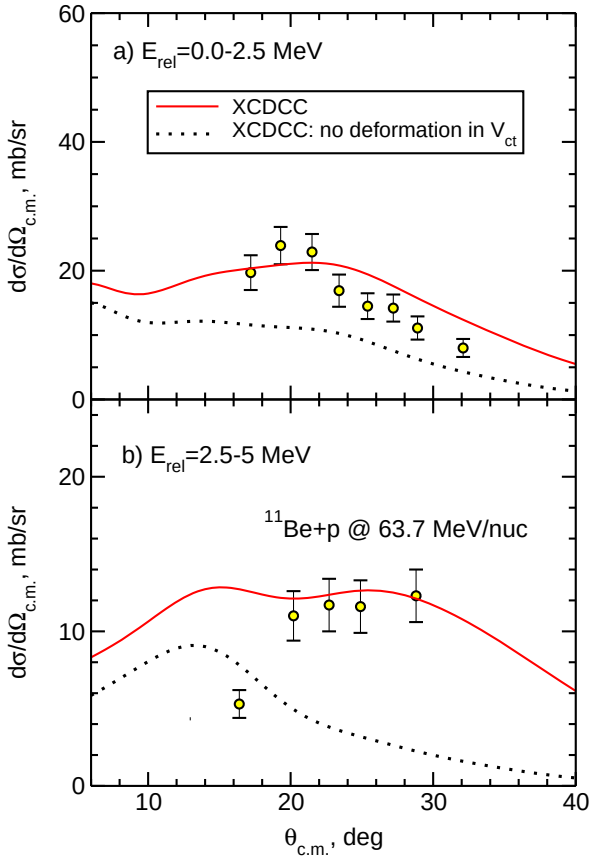

Figure 1. (Color online) Differential breakup cross sections, with respect to the outgoing ^{11}Be* c.m. scattering angle, for the breakup of ^{11}Be on protons at 63.7 MeV/nucleon. Upper and bottom panels correspond to the neutron-core relative energy intervals $E_{\rm rel}$ = 0–2.5 MeV and $E_{\rm rel}$ = 2.5–5 MeV, respectively.

For this purpose, we compare in Figure 2 two XCDCC calculations, with and without deformation in the ^{10}Be+^{64}Zn interaction, giving almost identical results. This indicates that the effect of the dynamical core excitation is very small in this case. We also note that these calculations, although using the same n+^{64}Zn and ^{10}Be+^{64}Zn potentials as those presented in Ref. [15], have been obtained after including higher partial waves and excitation energies in the continuum. The use of this augmented model space results in a slight improvement with the experimental data from Ref. [23].

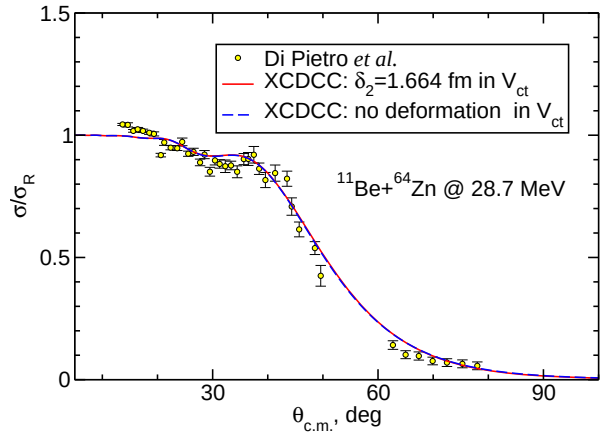

Figure 2. (Color online) Quasi-elastic differential cross section for ^{11}Be on ^{64}Zn at $E_{\rm lab}$=28.7 MeV, compared with XCDCC calculations.

4.3 ^{11}Be+ ^{208}Pb breakup

As a final example, we performed XCDCC calculations for the collision of ^{11}Be on a ^{208}Pb target at 69 MeV/nucleon, which corresponds to the energy of the experiment from RIKEN [24].

At these energies the breakup process connects the ground state directly with the breakup channels and, at the forward measured angles, the most strongly coupled states will be the $1/2^-$ and $3/2^-$. These states cannot be populated by the dynamic core excitation mechanism in first order because of the quadrupole nature of this excitation. As a result, for this reaction the main core-excitation effect is due to the presence of core-excitation admixtures in the projectile states.

The XCDCC calculations are compared with the data in Figure 3 corresponding to the breakup angular distribution, after integration over relative n-^{10}Be energies below 5 MeV. The solid line is the full calculation after convolution with the experimental angular resolution quoted in [24]. To illustrate the dominance of the dipole excitation mechanism, we have plotted also the separate contribution of the $1/2^{\pm}$, $3/2^{\pm}$ and $5/2^{\pm}$ states. It can be seen that, at sufficiently small angles, the breakup is largely dominated by the coupling to the dipole states. The calculation is found to be in very good agreement with the data without using any scaling factor.

The dominance of dipole Coulomb couplings can also be seen in Figure 4, where the differential energy cross section is plotted for two different angular ranges. In both intervals, the breakup process could be accounted for by using a pure $E1$ excitation mechanism even though two small bumps appear at $5/2^+$ and $3/2^+$ resonance energies for higher angles. These peaks are related to quadrupole contributions and they are washed out in the convoluted distribution because of the energy resolution.

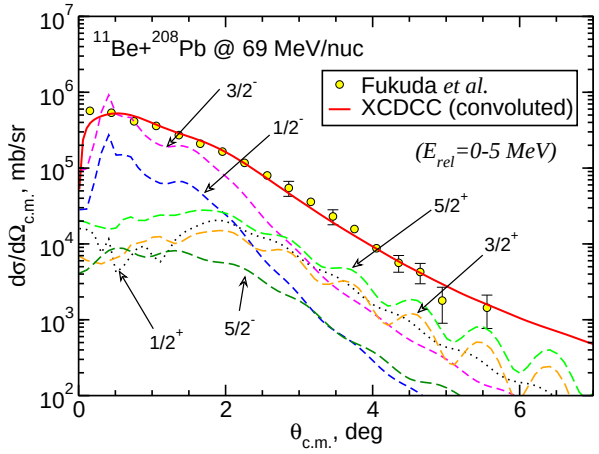

Figure 3. (Color online) Breakup differential cross section for ^{11}Be on ^{208}Pb at $E_{\rm lab}$ = 69 MeV/nucleon, integrated in the n-^{10}Be relative energy up to 5 MeV. The data are from Ref. [24]. The lines are XCDCC calculations described in the text. The full calculation (solid line) has been convoluted with the experimental angular resolution for a meaningful comparison with the data.

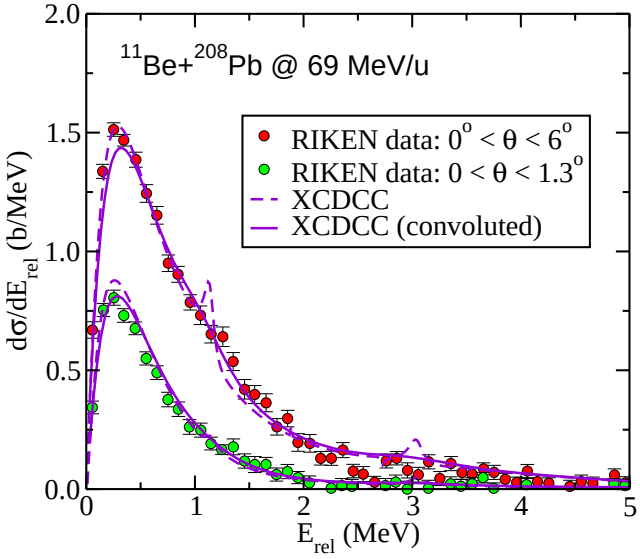

Figure 4. (Color online) Breakup differential energy cross section for ^{11}Be on ^{208}Pb at $E_{\rm lab}$ = 69 MeV/nucleon in the c.m. frame. The lines are XCDCC calculations before (dashed line) and after (solid line) convolution with the experimental energy resolution for a meaningful comparison with the data in Ref. [24].

5 Summary and Conclusions

To summarize, we have applied an extension of the CDCC formalism to the scattering of the two-body halo nucleus ^{11}Be on several inert targets: ^{1}H, ^{64}Zn and ^{208}Pb at 63.7 MeV/nucleon, 28.7 MeV, and 69 MeV/nucleon, respectively.

The projectile states are described in the weak-coupling limit so they are expanded as a superposition of products of single-particle configurations and core states. The continuum spectrum is discretized upon diagonalization of the hamiltonian in a basis of square-integrable functions. For the relative motion between the valence particle and the core, we use the analytical Transformed Harmonic Oscillator (THO) basis.

For the two-body projectile, we adopted a simple particle-rotor model, assuming a permanent axial core deformation in ^{10}Be, and the core-target interaction is obtained by deforming a central phenomenological potential. Therefore, the effect of core excitation is present in both the structure of the projectile and the dynamics of the reaction, through the non-central part of the potential.

In the ^{11}Be+p reaction, the calculations reproduce well the experimental breakup data. In particular, we confirm the importance of the dynamic core excitation mechanism for the excitation of the low-lying $5/2^+$ and $3/2^+$ resonances.

The ^{11}Be+^{64}Zn quasi-elastic cross section is well reproduced at all angles, except for some slight overestimation at $\theta_{\rm c.m} \approx 30^\circ$. For this medium-mass target and low incident projectile energy, unlike the proton target case, the dynamic core excitation mechanism is found to be small and the full calculations can be simulated using an optical core-target potential describing the corresponding elastic data.

Finally, the calculated breakup angular distribution for the reaction ^{11}Be + ^{208}Pb is found to reproduce very well the available data. For this heavy target, and at very small angles, the breakup is dominated by the dipole Coulomb couplings from the ground state to the $1/2^-$ and $3/2^-$ continuum states. Because these states cannot be populated by a direct core excitation mechanism, the effects of this excitation are restricted to the admixture of different core and valence configurations in the projectile wavefunctions.

Summarizing, the core-excitation is present in the structure of the projectile for all targets. However, the dynamic core excitation mechanism is only important for light targets (for which the dipole excitations are small compared to the quadrupole collective excitations of the core). Although all the calculations in this paper correspond to the ^{11}Be nucleus, we believe that the results are extrapolable to other weakly-bound nuclei.

Acknowledgements

This work has been partially supported by the Spanish Ministerio de Economía y Competitividad and FEDER funds under projects FIS2013-41994-P and FIS2014-

53448-C2-1-P. We also acknowledge funding from the European Union's Horizon 2020 research and innovation program under grant agreement No 654002. R.D. thanks support by the Fundação para a Ciência e a Tecnologia (FCT) through Grant No. SFRH/BPD/78606/2011.

References

[1] G.H. Rawitscher, *Phys. Rev. C* **9** (1974) 2210.
[2] N. Austern, Y. Iseri, M. Kamimura, M. Kawai, G. Rawitscher, and M. Yahiro, *Phys. Rep.* **154** (1987) 125.
[3] P. Banerjee and R. Shyam, *Phys. Rev. C* **61** (2000) 047301.
[4] J.A. Tostevin, S. Rugmai, and R.C. Johnson, *Phys. Rev. C* **57** (1998) 3225.
[5] L.D. Faddeev, *Zh. Eksp. Theor. Fiz.* **39** (1960) 1459.
[6] E.O. Alt, P. Grassberger, and W. Sandhas, *Nucl. Phys. B* **2** (1967) 167.
[7] S. Typel and G. Baur, *Phys. Rev. C* **50** (1994) 2104.
[8] H. Esbensen and G.F. Bertsch, *Nucl. Phys. A* **600** (1996) 37.
[9] T. Kido, K. Yabana, and Y. Suzuki, *Phys. Rev. C* **50** (1994) R1276.
[10] S. Typel and G. Baur, *Phys. Rev. C* **64** (2001) 024601.
[11] P. Capel, G. Goldstein, and D. Baye, *Phys. Rev. C* **70** (2004) 064605.
[12] A. García-Camacho, A. Bonaccorso, and D.M. Brink, *Nucl. Phys. A* **776** (2006) 118.
[13] N.C. Summers, F.M. Nunes, and I.J. Thompson, *Phys. Rev. C* **74** (2006) 014606.
[14] J.A. Lay, A.M. Moro, J.M. Arias, and J. Gómez-Camacho, *Phys. Rev. C* **85** (2012) 054618.
[15] R. de Diego, J.M. Arias, and A.M. Moro, *Phys. Rev. C* **89** (2014) 064609.
[16] J.A. Tostevin, F.M. Nunes, and I.J. Thompson, *Phys. Rev. C* **63** (2001) 024617.
[17] R. de Diego, R. Crespo, and A.M. Moro (in preparation).
[18] A. Bohr and B. Mottelson, *Nuclear Structure*, W. A. Benjamin, New York (1969).
[19] T. Tamura, *Rev. Mod. Phys.* **37** (1965) 679.
[20] S. Karataglidis, K. Amos, and B.G. Giraud, *Phys. Rev. C* **71** (2005) 064601.
[21] A. Shrivastava *et al.*, *Phys. Lett. B* **596** (2004) 54.
[22] R. Crespo, A. Deltuva, and A.M. Moro, *Phys. Rev. C* **83** (2011) 044622.
[23] A. Di Pietro *et al.*, *Phys. Rev. Lett.* **105** (2010) 022701.
[24] N. Fukuda *et al.*, *Phys. Rev. C* **70** (2004) 054606.